Available online at www.sciencedirect.com
ScienceDirect
Polymer 47 (2006) 8389–8399
polymer
www.elsevier.com/locate/polymer

Computationally designed monomers for molecular imprinting of chemical warfare agents – Part V

Dumitru Pavel [a,*], Jolanta Lagowski [a], Carmela Jackson Lepage [b]

[a] Department of Physics, Memorial University of Newfoundland, St. John's, NL, Canada
[b] Chemical Biological Defence Section, Defence R&D Canada – Suffield, AB, Canada

Received 7 May 2006; received in revised form 28 September 2006; accepted 30 September 2006
Available online 31 October 2006

Abstract

The main objective of this research is to develop and apply state-of-the-art computational tools to achieve an understanding of intermolecular interactions in molecular imprinting of chemical warfare (CW) agents into complex monomeric systems. Molecular dynamic (MD) simulations were carried out for different monomeric molecular systems in order to predict the interaction energies, the closest approach distances and the active site groups between the simulated molecular systems and different CW agents. The minimized structures of CW agents have been obtained with the use of molecular mechanics approach. NVT MD simulations at room temperature were carried out to obtain equilibrated conformations in all cases. The simulated molecular systems consisted of a ligand (CW agents) and commonly used functional monomers.

During this study, it was found that electrostatic interactions play the most significant role in the formation of molecular imprinting materials. The simulated systems indicate that the functional groups of monomers interacting with ligands tend to be either $-COOH$ or $CH_2{=}CH-$.

Keywords: Molecular imprinting technology; Molecular simulation; Warfare agents

1. Introduction

Molecular simulation techniques are playing an increasingly important role in the designing and the development of materials for various industrial applications. These simulations are likely to benefit the study of materials by increasing our understanding of their chemical and physical properties at molecular and atomic levels and by assisting us in the design of new materials and predicting their properties. Simulations are usually considerably cheaper and faster than laboratory experiments. Molecular simulations also offer a unique perspective on the molecular level processes controlling the structural, physical, optical, chemical, mechanical, and transport properties.

The main objective of this research is to apply state-of-the-art computational tools to achieve an understanding of intermolecular interactions in molecular systems that are employed in the imprinting of chemical warfare (CW) agents. This work is part of a larger study [1,2] to access the usefulness of computational aid in the development of imprinted monomers that can then be used for sensing industrially or militarily important compounds. In particular, this research is part of an exploratory investigation whose principal objective is to enhance the capabilities of first responders to determine the presence of hazardous chemical compounds in the environment. Its ultimate goal is the development of portable and direct sensing devices capable of detecting and identifying these hazardous materials [3–7].

Molecular imprinting is a technique of producing cavities in the material that preferentially bind with a particular molecule (template). In recent years the molecular imprinting

* Corresponding author. Present address: University of Sydney, Faculty of Pharmacy, Sydney, NSW 2006, Australia. Tel.: +61 2 93516066; fax: +61 2 93514391.
E-mail addresses: dumitru_p@yahoo.co.uk, dumitru@pharm.usyd.edu.au (D. Pavel).

0032-3861/$ - see front matter
doi:10.1016/j.polymer.2006.09.067

technique has focused on using synthetic polymers as imprinting material producing the so-called artificial recognition elements [8,9]. When compared with biomolecules, the main advantages of molecularly imprinted polymers (MIPs) are their relatively high stability over a wide range of conditions (temperature, pressure, organic solvents, etc.) and low cost. In other words, the artificial recognition elements (materials) provide an alternative to the use of the somewhat fragile biological elements (such as enzymes, proteins or antibodies), which lack storage, thermal and operational stabilities in the traditional sensing devices. Applications of imprinting technology are still very few and the field is relatively underdeveloped. Imprinting technology has a great potential for growth, for example, in the military, security, chemical, pharmaceutical and biotechnology industries [10–15].

Standard molecular imprinting is a process in which functional monomers, polymers or copolymers are allowed to self-assemble around a template molecule and then they are cross-linked into place [16–19]. The template is encapsulated in a stable three-dimensional polymer or copolymer matrix. The template molecule can then be removed, leaving behind a cavity that will bind molecules identical to the template molecule. The imprint is like a lock that is only compatible with the correct key, similar to biological systems, such as enzymes and substrates, antibodies and antigens, and hormones and receptors. Recognition between a molecular receptor (host) and a substrate (guest) in a matrix containing structurally related molecules requires discrimination and specific binding; this can happen only if the binding sites of the host and the guest molecules complement each other in size, shape, and chemical functionality. When these arrays are coupled with sensors employing standard surface analytical or photonic techniques, targeted species will be detectable and identifiable in real time.

In this work, MD simulations were carried out for different monomeric molecular systems (clusters) to assess the interaction energies, closest approach distances and the active site groups between the simulated molecular systems and different CW agents. The equilibrated structures of the simulated agents have been obtained with the use of molecular mechanics approach.

Simulated molecular systems consisted of a ligand and a monomer cluster which consists of 10 molecules of the studied monomers. The studied monomers are commonly used as functional monomers, such as acrylic acids, methacrylic acids, acrylamides, acroleins, acrylonitriles, styrenes, etc. (a total number of 25 different monomers were simulated, see Table 1). The initial conformations of each of the molecular systems were optimized and energy was minimized and presented in Appendix A. Then, NVT MD simulations for 40 ns at room temperature were carried out to obtain equilibrated conformations in order to analyse the imprinting properties. For each pair of molecular systems, a total energy difference, (ΔE), was calculated in order to estimate the interaction energy between ligand and the corresponding molecular cluster. Also, the closest distance between the active site (group) of the simulated monomeric molecular clusters and a ligand was estimated.

Table 1
List of simulated monomers

No	Functional monomer
1	1-Vinylimidazole
2	2-Vinylpyridine
3	2-Acrylamido-2-methyl-1-propanesulfonic acid
4	2-Hydroxyethyl methacrylate
5	Acrolein
6	Acrylamide
7	Acrylic acid
8	Acrylonitrile
9	Allylamine
10	Ethylene glycol dimethacrylate
11	Imidazole-4-acrylic acid ethyl ester
12	Methylenesuccinic acid
13	*m*-Divinylbenzene
14	*N*,*N*-Methylene-bis-acrylamide
15	Methacrylic acid
16	Imidazole-4-acrylic acid
17	4-Vinylpyridine
18	*p*-Divinylbenzene
19	Styrene
20	2-(Diethylamino)-ethyl methacrylate
21	Itaconic acid
22	Trifluoro-methacrylic acid
23	4-Vinylbenzoic acid
24	4-Vinylbenzyl-imino-di-acetic acid
25	4-Vinylimidazole

To our knowledge, there is very little theoretical/computational effort being carried out for the imprinting materials. Therefore, the present work is also exploratory in nature. We hope that the general methodology presented here can be applied to any molecularly imprinting material and become a reliable, economic and useful tool to aid the design and synthesis process of these special materials which can then be used in sensing applications.

1.1. Computational methodology

Computer modelling of chemical structures of the molecular clusters, molecular dynamic simulations, and conformational and molecular dynamic analyses were carried out using molecular simulation software for material science [20], Cerius^2 version 4.10 and Materials Studio designed by Accelrys. The 3D-Sketcher, Open Force-Field, charge equilibration, monomer editor, polymer builder, energy minimiser, NVT molecular dynamics (Discover) and dynamic analysis modules of Cerius^2 software were used in order to perform the computations and to calculate the binding energies (ΔE) and binding distances (d) between the simulated molecular systems (clusters) and different CW agents.

The Open Force-Field (OFF) module allowed the specification of the force field to be used for these simulations. The polymer consistent force-field (PCFF) implemented in Discover module was applied since it was found to be very suitable and reliable for the molecular simulation of organic molecular clusters (in this study for monomers) and polymers in accordance with previous studies [21–25]. This force field

is parameterized for a large class of organic molecules involving H, C, O, S, P, F, Cl and Br, allowing it to be applied to bio- and synthetic polymers. It was found that the PCFF force-field leads to accurate geometries for various polymeric systems [25] and can be used to calculate and minimise the energy of a simulated monomeric and polymeric systems. Next, the forces acting on each atom of a model polymer were calculated, which were then utilised to solve Newton's equations of motion for molecular dynamic simulations.

The initial molecular clusters were optimised and the value of the total potential energy and its components was obtained. The PCFF provides a potential energy interaction function (E_{total}) that accounts for both bonded (E_b) and non-bonded (E_{nb}) interactions. The bonded terms typically include harmonic bond stretching (E_s), harmonic angle bending (E_a), torsional (E_t), and inversion (E_i) energies. Non-bonded terms typically contain van der Waals (E_{vdW}), electrostatic (Coulombic) (E_q) and hydrogen bond (10-12 potential) (E_{hb}) interactions. In practice it is common to use a suitably large cut-off distance. For this study a cut-off distance of 100 Å was used for non-bonded interactions, with this cut-off distance all the non-bonded interactions of the simulated molecular clusters are calculated. The 6-12 potential [26], that is often referred to in the literature as the Lennard–Jones 6-12 potential function ($u = A/r^{12} - B/r^6$), was used to calculate the non-bonded van der Waals interactions. A and B are parameters which determine the size of the attraction ($-B/r^6$) and repulsion (A/r^{12}) interactions between the atoms which are separated by a distance r equal to the sum of r_i and r_j, where r_i and r_j are van der Waals radii of the non-bonded atoms i and j.

The charge distribution in the molecule, due to Coulombic (electrostatic) interactions, of the simulated molecular clusters was obtained with the charge equilibration method that is available in the Cerius^2 molecular simulation software for material science [20,27]. The validity of the molecular simulation calculations depends on the suitability and accuracy of the equations used for the bonded and non-bonded potentials which are of great importance for industrial applications.

The NVT molecular dynamic simulations were performed at 300 K, for each constructed and minimised molecular system. For the NVT ensemble, the number of molecules N, volume V and the temperature T of the system are kept constant. Molecular dynamic (MD) calculations simulate the natural motions of all atoms in a molecular system over time at non-zero temperature and the MD algorithm makes use of Newton's equation of motion ($F = ma$), thus giving a complete dynamic description of the simulated molecular cluster. In order to ensure that the simulations are carried out for sufficient time, which is one of the most important criteria in equilibrating the system and then to accurately predict its properties, the simulation time of NVT MD calculations was set between 30 ns and 40 ns, depending on the size of the simulated molecular system, and the output frequency was calculated for every 2000 steps. The time step of 0.001 ps is taken to be constant for all the simulations of this study. In this study the model system exchanges energy with a heat bath in order to maintain a constant temperature. The non-canonical 'T-damping' thermostat was used for isothermal–isobaric NVT MD simulations [28]. For all the simulations the dielectrical constant was kept constant at a value of 1. Trajectory file data generated from NVT MD simulation has been used in all the calculations and analyses (including visual analysis as well) presented in this research. The trajectory files were analysed by dynamic analysis modules. More details about computational procedure are presented in our previous work [1,2].

2. Computer modelling of chemical warfare agents

In order to build up a virtual library of host–guest systems, we have performed simulations for CW agents as listed in Table 2. The main objectives of this study were to perform MD simulations for different molecular systems in order to predict the interaction (binding) energies, binding distance and the active site groups between the simulated molecular systems and different CW agents, and to determine which one would be the best candidate for imprinting technology.

The binding distance is an average value of the close contacts of the chemical agent and the simulated monomers. As previously observed [1,2], in most cases, the functional groups of monomers interacting with ligands (CW agents) tend to be either –COOH or CH_2=CH–. In majority of cases (see Ref. [29] and references within and others [8,9,30,31]), the synthesis of molecularly imprinting polymers involves polymerization of monomers in the presence of a cross-linker. This means that CH_2=CH– groups would not be present when the imprinted cavity was formed. From our previous computational/theoretical work [1] which investigated H-bonds between monomers (methacrylic acid) and ligand (theophylline) using quantum mechanical approach (see *Figures 13–15* in Ref. [1]) as well as carrying out MD simulations, it is clear that –COOH group plays the dominant role in coming closest and hence interacting strongest with the ligand. As an aside it can be noted that this simulation also indicates that CH_2=CH– (and of course –COOH) groups promote stronger interactions between monomers themselves, hence in affect the functional groups aid in the formation of a network of monomers around the ligand; monomers can then be polymerised and/or cross-linked. For example, see Fig. 1 which illustrates the interactions of –COOH and CH_2=CH– groups of methacrylic acids with hydrocyanic acid and between themselves.

From experiments [29], it is known that the most important factor in choosing the monomers for the imprinting process is the monomer–ligand functional group complementarity, for example, when ligand contains H-bond donating groups, monomers should contain H-bond accepting groups, etc. Furthermore, a survey contained in Ref. [29] illustrates that most of the functional monomers used in non-covalent imprinting with various templates give good rebinding selectivity, clearly implying that the dominant functional groups of monomers must be other than CH_2=CH– group (such as –COOH for example) since in all cases upon polymerization majority of CH_2=CH– would not be present. In fact, in one experimental study of theophylline MIP [30] it was (indirectly) shown that

Table 2
A list of simulated chemical warfare agents

CW agent class		Common name[a] (identifier)	Chemical Abstracts Service (CAS) name	Chemical structure
Blood agents		(CK)	Cyanogen chloride	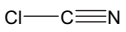
		Hydrogen cyanide (AC)	Hydrocyanic acid	
Choking agents		(Cl)	Chlorine	
		Phosgene (CG)	Carbonic dichloride	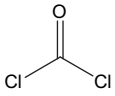
Nerve agents	G-series	Tabun (GA)	Dimethylphosphoroamidocyanidic acid, ethyl ester	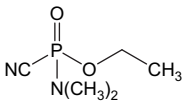
		Sarin (GB)	Methylphosphonofluoridic acid, (1-methylethyl) ester	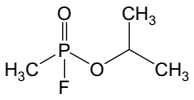
		Soman (GD)	Methylphosphonofluoridic acid, 1,2,2-trimethylpropyl ester	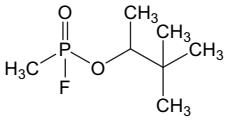
		Cyclohexyl sarin (GF)	Methylphosphonofluoridic acid, cyclohexyl ester	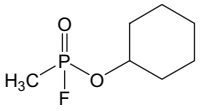
	V-series	(VX)	Methylphosphonothioic acid, *S*-[2-[bis(1-methylethyl)-amino]ethyl]-*O*-ethyl ester	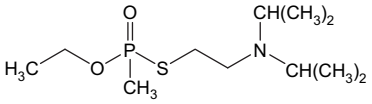
Blister agents		Mustard (H)	1,1′-Thiobis[2-chloroethane]	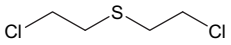
		Lewisite (L)	(2-Chloroethenyl)-arsonous dichloride	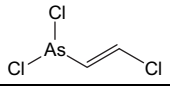

[a] If different from CAS name.

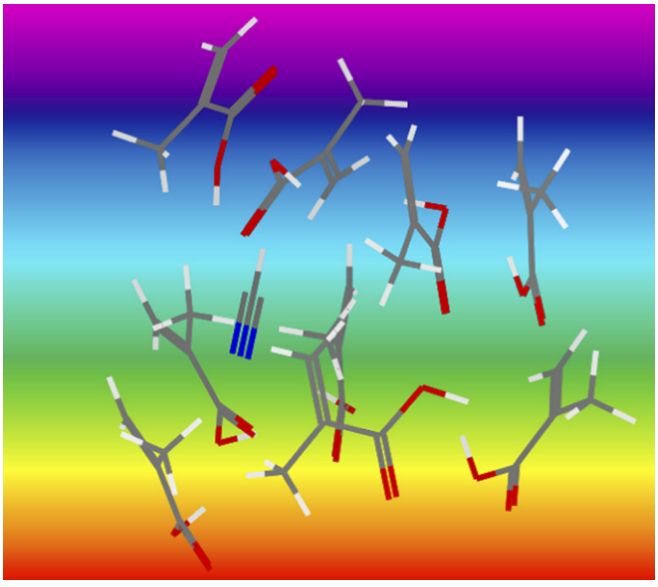

Fig. 1. A typical example of the simulated molecular cluster containing 10 molecules of methacrylic acid and 1 molecule of hydrocyanic acid.

−COOH groups must be the key to the formation of stable and selective imprinting cavities since the process of decarboxylation initiated at higher temperatures (above 150 °C) led to loss of affinity for the template (theophylline in this case). Yet, in another investigation [32] it is shown that increasing the amount of template does not lead to indefinite increase in number of binding sites; this is explained by the differences in complexes formed by the template and monomer(s) whose functional groups were again −COOHs. More recently, another experimental study [33] illustrated that an improvement of binding sites' properties can be achieved by ionization state selective modification of −COOH groups in MIPs. In summary, CH_2=CH− may initially play some role in the formation of H-bonds with the ligand (and other monomers), however, upon polymerization other functional groups are sufficient to form imprinting cavities with good selective rebinding capability.

The interaction energy, ΔE, was calculated as follows:

$$\Delta E = E_{\text{cluster}} - \left(E_{\text{monomer}} + E_{\text{chemical warfare agent}}\right)$$

where, $E_{cluster}$, is the total energy of the simulated cluster (monomers and CW agent), $E_{monomer}$ is the total energy of the monomers and $E_{chemical\ warfare\ agent}$ is the total energy of the given CW agent. There are a number of reasons why ΔE might be a good quantity to use in evaluating the properties of possible MIPs. In one study [17] that combines the computational approach with experimental evidence, it is shown that higher binding (interaction) energy between monomers and template (computed as shown above) leads to more stable complexes in the prepolymerization stage which, in turn, results in binding sites with higher binding affinity in the imprinted polymers. In fact, most of MIP studies [8,17,32,34] focus strongly on the stability of the template–monomer complex before polymerization. In these studies, it is shown that there is a strong correlation between the number of binding sites with high affinity and specificity and the stability and the extent of the molecular cluster consisting of monomers and template before polymerization (see Ref. [17] and references within). In another study [8] it was shown that monomer–template complexes with highest binding scores (as obtained from the empirical binding score function) followed by simulated annealing can also lead to better rational design of MIP with enhanced selectivity for creatinine. Binding scores are based on the empirical Gibbs free energy differences, ΔG [35,36] which may consist of many terms including van der Waals interaction, hydrogen bonding, deformation penalty and hydrophobic effect [35]. These empirical scoring functions are not derived from 'first principles' and must use an experimentally obtained data to determine the various parameters used in ΔG expression. The most extensive research has gone into scoring functions for the protein–ligand imprinting driven by the need to advance the structure-based drug design [37,38]. Similar efforts have not been made for the industrial (synthetic) polymers [35]. It should be pointed out that the interaction energy is an approximation to the enthalpy change or the free energy change in the binding process and hence is a physically significant quantity. Therefore, it appears that at this time calculations of direct interaction energies, ΔE, in MD simulations are a reasonable choice for predicting binding affinities of MIPs and templates. That is, based on the above factors, we can conclude that a large negative value of ΔE for a given monomer–CW agent cluster should give a good indication that this particular monomer will form stable complex with that CW agent and will be a good candidate for MIP. Of course, a final confirmation must come from experimental investigation.

The binding distance and binding energy of simulated monomers to cyanogen chloride (CK) are presented in Table 3. CK gives roughly equivalent bindings with itaconic acid, imidazole-4-acrylic acid ethyl ester, methacrylic acid, 4-vinylpyridine and 2-hydroxyethyl methacrylate.

The binding distance and binding energy of simulated monomers to hydrogen cyanide (AC) are presented in Table 4. The most stable binding for AC occurs with 2-acrylamido-2-methyl-1-propanesulfonic acid.

The binding distance and binding energy of simulated monomers to chlorine are presented in Table 5. 4-Vinylpyridine forms the most stable complex with chlorine.

Table 3
Binding distance and binding energy of simulated monomers to cyanogen chloride (CK)

No	Functional monomer	Distance (Å)	ΔE (kcal/mol)
1	1-Vinylimidazole	2.11	28
2	2-Vinylpyridine	2.47	12
3	2-Acrylamido-2-methyl-1-propanesulfonic acid	1.89	67
4	2-Hydroxyethyl methacrylate	2.58	−19
5	Acrolein	2.42	65
6	Acrylamide	3.45	48
7	Acrylic acid	2.11	13
8	Acrylonitrile	2.34	23
9	Allylamine	3.45	85
10	Ethylene glycol dimethacrylate	2.54	−6
11	Imidazole-4-acrylic acid ethyl ester	1.83	−27
12	Methylenesuccinic acid	2.08	120
13	*m*-Divinylbenzene	2.11	75
14	*N*,*N*-Methylene-bis-acrylamide	3.26	69
15	Methacrylic acid	2.47	−26
16	Imidazole-4-acrylic acid	3.75	58
17	4-Vinylpyridine	3.12	−22
18	*p*-Divinylbenzene	2.38	90
19	Styrene	2.95	78
20	2-(Diethylamino)ethyl methacrylate	2.48	119
21	Itaconic acid	1.98	−32
22	Trifluoro-methacrylic acid	2.03	20
23	4-Vinylbenzoic acid	3.01	103
24	4-Vinylbenzyl-imino-di-acetic acid	2.97	68
25	4-Vinylimidazole	2.75	35

Table 4
Binding distance and binding energy of simulated monomers to hydrogen cyanide (AC)

No	Functional monomer	Distance (Å)	ΔE (kcal/mol)
1	1-Vinylimidazole	2.45	154
2	2-Vinylpyridine	2.67	37
3	2-Acrylamido-2-methyl-1-propanesulfonic acid	1.94	−258
4	2-Hydroxyethyl methacrylate	3.06	127
5	Acrolein	3.83	57
6	Acrylamide	2.56	102
7	Acrylic acid	2.06	79
8	Acrylonitrile	2.34	25
9	Allylamine	3.05	142
10	Ethylene glycol dimethacrylate	2.67	−18
11	Imidazole-4-acrylic acid ethyl ester	2.32	179
12	Methylenesuccinic acid	3.24	47
13	*m*-Divinylbenzene	2.87	269
14	*N*,*N*-Methylene-bis-acrylamide	2.28	−32
15	Methacrylic acid	3.15	84
16	Imidazole-4-acrylic acid	3.68	126
17	4-Vinylpyridine	4.10	270
18	*p*-Divinylbenzene	3.91	241
19	Styrene	4.09	184
20	2-(Diethylamino)ethyl methacrylate	2.02	13
21	Itaconic acid	3.13	385
22	Trifluoro-methacrylic acid	3.74	283
23	4-Vinylbenzoic acid	3.61	316
24	4-Vinylbenzyl-imino-di-acetic acid	3.80	149
25	4-Vinylimidazole	4.37	67

Table 5
Binding distance and binding energy of simulated monomers to chlorine

No	Functional monomer	Distance (Å)	ΔE (kcal/mol)
1	1-Vinylimidazole	2.04	−5
2	2-Vinylpyridine	2.11	14
3	2-Acrylamido-2-methyl-1-propanesulfonic acid	1.20	19
4	2-Hydroxyethyl methacrylate	2.15	29
5	Acrolein	2.71	−29
6	Acrylamide	2.05	57
7	Acrylic acid	2.73	45
8	Acrylonitrile	2.16	45
9	Allylamine	2.07	6
10	Ethylene glycol dimethacrylate	2.36	16
11	Imidazole-4-acrylic acid ethyl ester	2.70	84
12	Methylenesuccinic acid	2.81	70
13	*m*-Divinylbenzene	2.17	37
14	*N*,*N*-Methylene-bis-acrylamide	2.10	13
15	Methacrylic acid	2.15	45
16	Imidazole-4-acrylic acid	2.40	13
17	4-Vinylpyridine	1.99	−53
18	*p*-Divinylbenzene	2.43	39
19	Styrene	3.15	118
20	2-(Diethylamino)ethyl methacrylate	2.43	75
21	Itaconic acid	2.83	31
22	Trifluoro-methacrylic acid	2.11	29
23	4-Vinylbenzoic acid	3.07	93
24	4-Vinylbenzyl-imino-di-acetic acid	2.19	9
25	4-Vinylimidazole	2.56	24

Table 6
Binding distance and binding energy of simulated monomers to phosgene (CG)

No	Functional monomer	Distance (Å)	ΔE (kcal/mol)
1	1-Vinylimidazole	2.20	125
2	2-Vinylpyridine	2.61	−20
3	2-Acrylamido-2-methyl-1-propanesulfonic acid	3.41	97
4	2-Hydroxyethyl methacrylate	3.20	250
5	Acrolein	3.52	133
6	Acrylamide	2.82	215
7	Acrylic acid	3.12	199
8	Acrylonitrile	3.50	270
9	Allylamine	3.74	285
10	Ethylene glycol dimethacrylate	3.51	189
11	Imidazole-4-acrylic acid ethyl ester	2.84	−75
12	Methylenesuccinic acid	2.45	−15
13	*m*-Divinylbenzene	3.49	280
14	*N*,*N*-Methylene-bis-acrylamide	3.37	157
15	Methacrylic acid	2.87	143
16	Imidazole-4-acrylic acid	3.90	251
17	4-Vinylpyridine	3.15	119
18	*p*-Divinylbenzene	3.70	204
19	Styrene	2.50	39
20	2-(Diethylamino)ethyl methacrylate	2.80	−203
21	Itaconic acid	4.15	−95
22	Trifluoro-methacrylic acid	3.79	180
23	4-Vinylbenzoic acid	3.55	215
24	4-Vinylbenzyl-imino-di-acetic acid	3.87	128
25	4-Vinylimidazole	4.17	239

The binding distance and binding energy of simulated monomers to phosgene (CG) are presented in Table 6. The most stable binding for phosgene occurs with 2-(diethylamino)ethyl methacrylate.

The binding distance and binding energy of simulated monomers to tabun (GA) are presented in Table 7. 2-Acrylamido-2-methyl-1-propanesulfonic acid gives the most stable complex with tabun.

The binding distance and binding energy of simulated monomers to sarin (GB) are presented in Table 8. Ethylene glycol dimethacrylate forms the most stable complex with sarin.

The binding distance and binding energy of simulated monomers to soman (GD) are presented in Table 9. The most stable complexes for soman occur with 4-vinylbenzyl-imino-di-acetic acid, *N*,*N*-methylene-bis-acrylamide and acrolein.

The binding distance and binding energy of simulated monomers to cyclohexyl sarin (GF) are presented in Table 10. Cyclohexyl sarin forms the most stable complex with acrylamide.

The binding distance and binding energy of simulated monomers to methylphosphonothioic acid-*S*-[2-[bis(1-methylethyl)amino]ethyl]-*O*-ethyl ester (VX) are presented in Table 11. Ethylene glycol dimethacrylate, 2-hydroxyethyl methacrylate, trifluoro-methacrylic acid and 4-vinylbenzoic acid all form stable complexes with VX with approximately the same strength.

Table 7
Binding distance and binding energy of simulated monomers to tabun (GA)

No	Functional monomer	Distance (Å)	ΔE (kcal/mol)
1	1-Vinylimidazole	3.51	229
2	2-Vinylpyridine	3.81	493
3	2-Acrylamido-2-methyl-1-propanesulfonic acid	2.10	−415
4	2-Hydroxyethyl methacrylate	3.42	59
5	Acrolein	3.82	140
6	Acrylamide	2.10	102
7	Acrylic acid	2.24	14
8	Acrylonitrile	2.03	−28
9	Allylamine	3.97	328
10	Ethylene glycol dimethacrylate	3.58	269
11	Imidazole-4-acrylic acid ethyl ester	2.56	77
12	Methylenesuccinic acid	2.02	−150
13	*m*-Divinylbenzene	4.02	323
14	*N*,*N*-Methylene-bis-acrylamide	3.32	80
15	Methacrylic acid	1.87	−32
16	Imidazole-4-acrylic acid	3.81	254
17	4-Vinylpyridine	3.76	286
18	*p*-Divinylbenzene	2.71	118
19	Styrene	3.58	198
20	2-(Diethylamino)ethyl methacrylate	2.10	−39
21	Itaconic acid	3.12	46
22	Trifluoro-methacrylic acid	3.20	195
23	4-Vinylbenzoic acid	3.64	453
24	4-Vinylbenzyl-imino-di-acetic acid	2.71	28
25	4-Vinylimidazole	3.83	269

Table 8
Binding distance and binding energy of simulated monomers to sarin (GB)

No	Functional monomer	Distance (Å)	ΔE (kcal/mol)
1	1-Vinylimidazole	2.67	86
2	2-Vinylpyridine	2.65	38
3	2-Acrylamido-2-methyl-1-propanesulfonic acid	2.46	380
4	2-Hydroxyethyl methacrylate	3.01	78
5	Acrolein	3.14	80
6	Acrylamide	2.62	62
7	Acrylic acid	2.37	193
8	Acrylonitrile	2.16	136
9	Allylamine	3.32	267
10	Ethylene glycol dimethacrylate	2.04	−185
11	Imidazole-4-acrylic acid ethyl ester	3.54	428
12	Methylenesuccinic acid	4.05	56
13	*m*-Divinylbenzene	3.58	410
14	*N*,*N*-Methylene-bis-acrylamide	2.13	−69
15	Methacrylic acid	4.24	317
16	Imidazole-4-acrylic acid	4.03	372
17	4-Vinylpyridine	3.92	396
18	*p*-Divinylbenzene	4.57	429
19	Styrene	5.10	358
20	2-(Diethylamino)ethyl methacrylate	3.87	176
21	Itaconic acid	3.97	414
22	Trifluoro-methacrylic acid	2.12	−29
23	4-Vinylbenzoic acid	3.08	241
24	4-Vinylbenzyl-imino-di-acetic acid	2.17	20
25	4-Vinylimidazole	2.28	41

The binding distance and binding energy of simulated monomers to mustard (H) are presented in Table 12. 2-Acrylamido-2-methyl-1-propanesulfonic acid forms the most stable complex with mustard.

Table 9
Binding distance and binding energy of simulated monomers to soman (GD)

No	Functional monomer	Distance (Å)	ΔE (kcal/mol)
1	1-Vinylimidazole	4.15	273
2	2-Vinylpyridine	3.72	87
3	2-Acrylamido-2-methyl-1-propanesulfonic acid	2.88	418
4	2-Hydroxyethyl methacrylate	2.54	230
5	Acrolein	2.01	−125
6	Acrylamide	3.41	82
7	Acrylic acid	2.26	20
8	Acrylonitrile	3.94	253
9	Allylamine	3.32	57
10	Ethylene glycol dimethacrylate	2.57	−65
11	Imidazole-4-acrylic acid ethyl ester	3.81	268
12	Methylenesuccinic acid	4.01	227
13	*m*-Divinylbenzene	3.48	301
14	*N*,*N*-Methylene-bis-acrylamide	1.94	−151
15	Methacrylic acid	3.37	134
16	Imidazole-4-acrylic acid	3.54	396
17	4-Vinylpyridine	4.38	426
18	*p*-Divinylbenzene	2.18	−62
19	Styrene	2.49	147
20	2-(Diethylamino)ethyl methacrylate	3.69	586
21	Itaconic acid	2.38	−7
22	Trifluoro-methacrylic acid	3.97	75
23	4-Vinylbenzoic acid	3.72	459
24	4-Vinylbenzyl-imino-di-acetic acid	2.11	−161
25	4-Vinylimidazole	3.38	353

Table 10
Binding distance and binding energy of simulated monomers to cyclohexyl sarin (GF)

No	Functional monomer	Distance (Å)	ΔE (kcal/mol)
1	1-Vinylimidazole	3.57	385
2	2-Vinylpyridine	2.37	24
3	2-Acrylamido-2-methyl-1-propanesulfonic acid	3.75	182
4	2-Hydroxyethyl methacrylate	2.06	−47
5	Acrolein	4.10	461
6	Acrylamide	3.38	−236
7	Acrylic acid	3.57	291
8	Acrylonitrile	2.30	51
9	Allylamine	2.28	263
10	Ethylene glycol dimethacrylate	3.60	412
11	Imidazole-4-acrylic acid ethyl ester	2.08	−91
12	Methylenesuccinic acid	3.75	259
13	*m*-Divinylbenzene	4.16	738
14	*N*,*N*-Methylene-bis-acrylamide	3.05	197
15	Methacrylic acid	2.69	201
16	Imidazole-4-acrylic acid	3.42	276
17	4-Vinylpyridine	2.59	15
18	*p*-Divinylbenzene	4.02	416
19	Styrene	5.04	938
20	2-(Diethylamino)ethyl methacrylate	2.03	−87
21	Itaconic acid	4.15	325
22	Trifluoro-methacrylic acid	2.90	171
23	4-Vinylbenzoic acid	3.64	235
24	4-Vinylbenzyl-imino-di-acetic acid	3.83	419
25	4-Vinylimidazole	3.75	258

The binding distance and binding energy of simulated monomers to lewisite (L) are presented in Table 13. 2-(Diethylamino)ethyl methacrylate and *N*,*N*-methylene-bis-acrylamide form the most stable complexes with lewisite.

Table 11
Binding distance and binding energy of simulated monomers to VX

No	Functional monomer	Distance (Å)	ΔE (kcal/mol)
1	1-Vinylimidazole	4.33	421
2	2-Vinylpyridine	3.96	273
3	2-Acrylamido-2-methyl-1-propanesulfonic acid	2.03	−9
4	2-Hydroxyethyl methacrylate	2.40	−56
5	Acrolein	4.67	328
6	Acrylamide	3.31	256
7	Acrylic acid	3.75	136
8	Acrylonitrile	3.81	492
9	Allylamine	2.79	17
10	Ethylene glycol dimethacrylate	2.69	−66
11	Imidazole-4-acrylic acid ethyl ester	4.23	287
12	Methylenesuccinic acid	3.28	358
13	*m*-Divinylbenzene	4.20	396
14	*N*,*N*-Methylene-bis-acrylamide	2.13	162
15	Methacrylic acid	3.75	170
16	Imidazole-4-acrylic acid	2.42	78
17	4-Vinylpyridine	4.51	192
18	*p*-Divinylbenzene	4.79	430
19	Styrene	2.14	399
20	2-(Diethylamino)ethyl methacrylate	4.17	495
21	Itaconic acid	3.94	220
22	Trifluoro-methacrylic acid	2.15	−40
23	4-Vinylbenzoic acid	3.32	−28
24	4-Vinylbenzyl-imino-di-acetic acid	3.72	60
25	4-Vinylimidazole	4.54	423

Table 12
Binding distance and binding energy of simulated monomers to mustard (H)

No	Functional monomer	Distance (Å)	ΔE (kcal/mol)
1	1-Vinylimidazole	3.12	110
2	2-Vinylpyridine	2.80	−53
3	2-Acrylamido-2-methyl-1-propanesulfonic acid	2.35	−195
4	2-Hydroxyethyl methacrylate	3.11	186
5	Acrolein	3.80	72
6	Acrylamide	3.71	140
7	Acrylic acid	2.92	−37
8	Acrylonitrile	3.64	492
9	Allylamine	2.70	−22
10	Ethylene glycol dimethacrylate	2.30	135
11	Imidazole-4-acrylic acid ethyl ester	4.03	310
12	Methylenesuccinic acid	2.15	−50
13	*m*-Divinylbenzene	3.21	359
14	*N*,*N*-Methylene-bis-acrylamide	2.35	69
15	Methacrylic acid	4.37	412
16	Imidazole-4-acrylic acid	2.57	60
17	4-Vinylpyridine	3.15	230
18	*p*-Divinylbenzene	3.52	48
19	Styrene	3.93	520
20	2-(Diethylamino)ethyl methacrylate	4.57	378
21	Itaconic acid	2.63	−52
22	Trifluoro-methacrylic acid	2.69	64
23	4-Vinylbenzoic acid	2.93	94
24	4-Vinylbenzyl-imino-di-acetic acid	2.52	74
25	4-Vinylimidazole	4.05	382

Table 13
Binding distance and binding energy of simulated monomers to lewisite (L)

No	Functional monomer	Distance (Å)	ΔE (kcal/mol)
1	1-Vinylimidazole	4.50	515
2	2-Vinylpyridine	4.42	819
3	2-Acrylamido-2-methyl-1-propanesulfonic acid	2.82	27
4	2-Hydroxyethyl methacrylate	3.60	420
5	Acrolein	3.67	178
6	Acrylamide	2.20	29
7	Acrylic acid	3.15	147
8	Acrylonitrile	3.87	479
9	Allylamine	2.58	142
10	Ethylene glycol dimethacrylate	2.25	384
11	Imidazole-4-acrylic acid ethyl ester	2.18	246
12	Methylenesuccinic acid	3.17	310
13	*m*-Divinylbenzene	2.51	42
14	*N*,*N*-Methylene-bis-acrylamide	2.09	−74
15	Methacrylic acid	2.72	171
16	Imidazole-4-acrylic acid	4.19	818
17	4-Vinylpyridine	3.75	279
18	*p*-Divinylbenzene	2.64	470
19	Styrene	2.43	113
20	2-(Diethylamino)ethyl methacrylate	2.14	−83
21	Itaconic acid	2.95	485
22	Trifluoro-methacrylic acid	3.54	286
23	4-Vinylbenzoic acid	2.72	51
24	4-Vinylbenzyl-imino-di-acetic acid	2.77	278
25	4-Vinylimidazole	2.18	55

3. Summary and conclusions

Atomistic modelling is a useful tool for studying the microscopic structure and understanding the mechanisms of physical processes on atomic and molecular levels. Molecular simulations of material structure have reached the level where they are now useful in gaining insights into the molecular origins of behaviour of bulk polymers. In the present work several molecular clusters have been investigated by extensive NVT MD simulations in order to obtain a better insight about the molecular imprinting formation, mechanism and properties. Extended equilibration procedures were necessary to obtain reasonable imprinting models for the simulated molecular clusters and the following conclusions were drawn.

For CW agents it was found that the most stable binding for:

- CK occurs with itaconic acid, imidazole-4-acrylic acid ethyl ester, methacrylic acid, 4-vinylpyridine and 2-hydroxyethyl methacrylate;
- AC with 2-acrylamido-2-methyl-1-propanesulfonic acid;
- Cl with 4-vinylpyridine;
- CG with 2-(diethylamino)ethyl methacrylate;
- GA with 2-acrylamido-2-methyl-1-propanesulfonic acid;
- GB with ethylene glycol dimethacrylate;
- GD with 4-vinylbenzyl-imino-di-acetic acid, *N*,*N*-methylene-bis-acrylamide and acrolein;
- GF with acrylamide;
- VX with ethylene glycol dimethacrylate, 2-hydroxyethyl methacrylate, trifluoro-methacrylic acid and 4-vinylbenzyl-imino-di-acetic acid;
- H with 2-acrylamido-2-methyl-1-propanesulfonic acid;
- L with 2-(diethylamino)ethyl methacrylate and *N*,*N*-methylene-bis-acrylamide.

Acknowledgments

This work is part of a CRTI project. CRTI is an initiative of the Canadian federal government aimed at providing new knowledge, technology, and research necessary for CBRN (Chemical, Biological, Radiological and Nuclear) response and preparedness. See: http://www.crti.drdc-rddc.gc.ca/.

Appendix A

The energy minimised structures of the simulated monomers.

A.1. Notes

The atoms color of all of the simulated molecular systems presented throughout this manuscript are as following:

Carbon	Grey
Hydrogen	Green
Oxygen	Red
Nitrogen	Blue
Sulfur	Yellow
Fluorine	Light blue

For interpretation of the references to color, the reader is referred to the web version of this article.

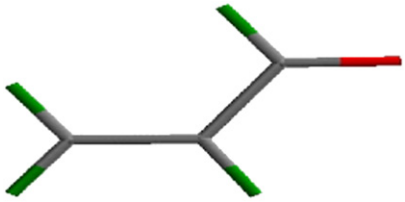

Acrolein

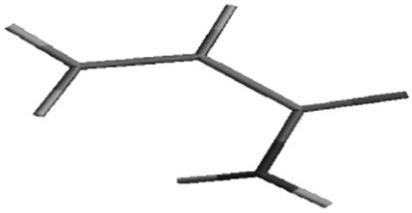

Acrylamide

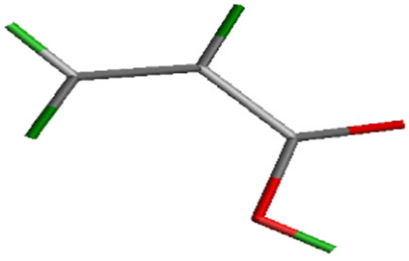

Acrylic acid

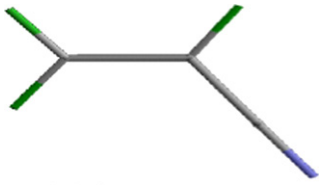

Acrylonitrile

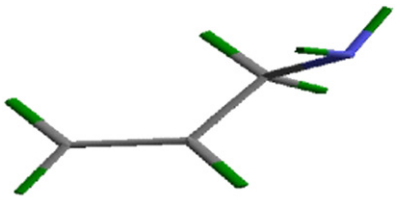

Allylamine

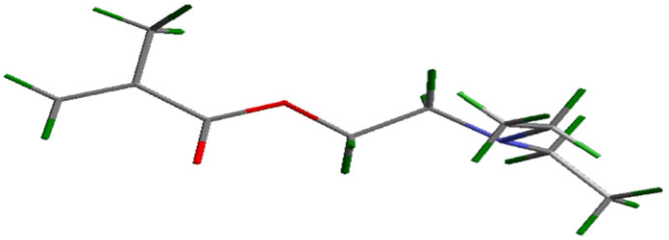

2-(Diethylamino)ethyl methacrylate

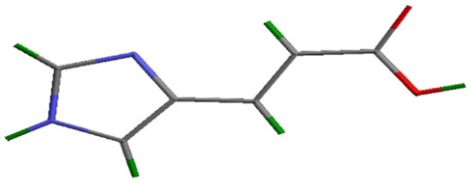

Imidazole-4-acrylic acid

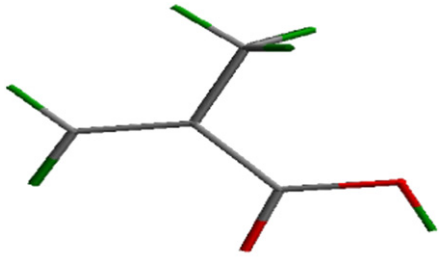

Methacrylic acid

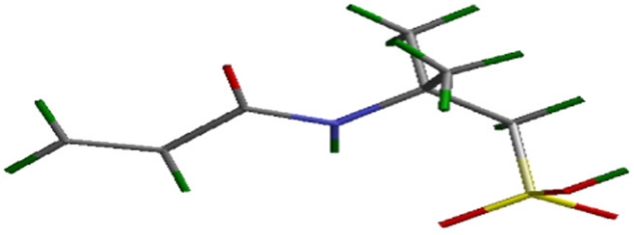

2-Acrylamido-2-methyl-1-propanesulfonic acid

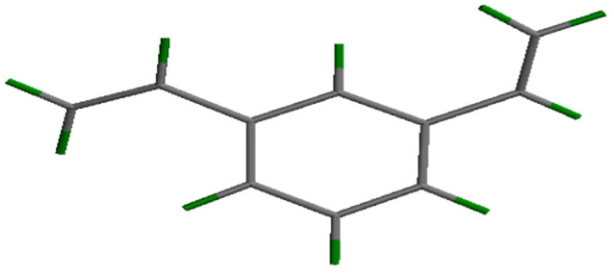

m-Divinylbenzene

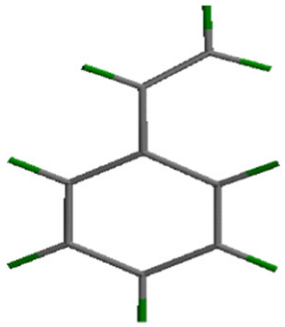

Styrene

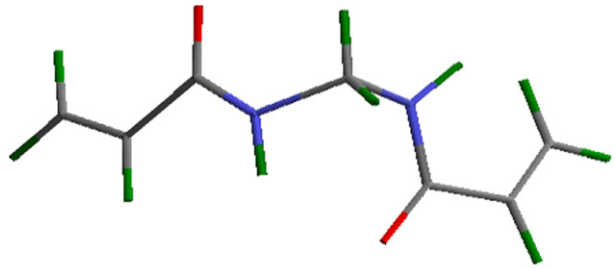

N,*N*-Methylene-bis-acrylamide

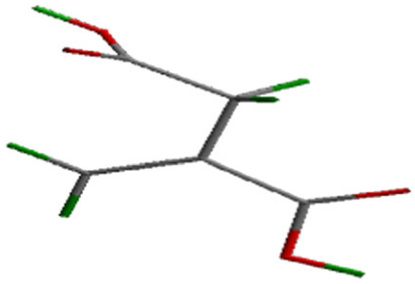

Methylenesuccinic acid

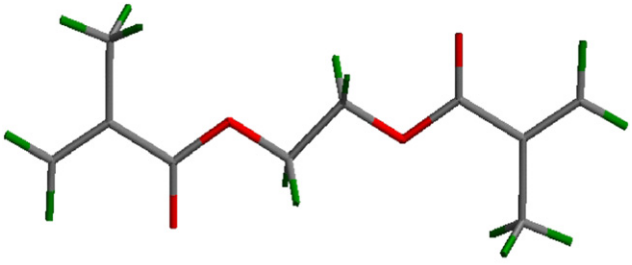

Ethylene glycol dimethacrylate

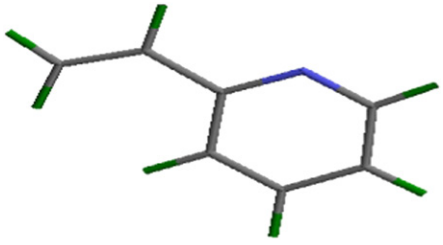

2-Vinylpyridine

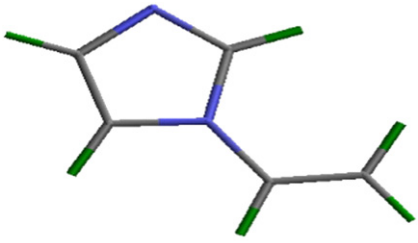

4-Vinylimidazole

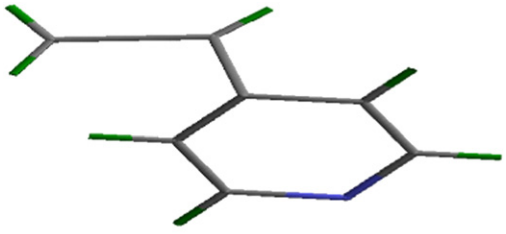

4-Vinylpyridine

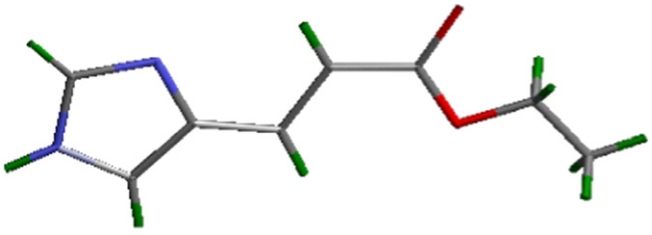

Imidazole-4-acrylic acid ethyl ester

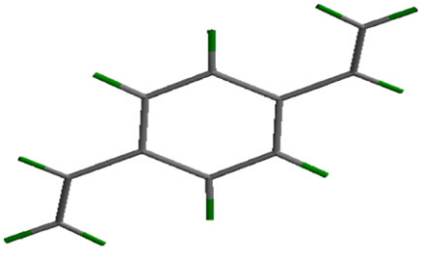

para-Divinylbenzene

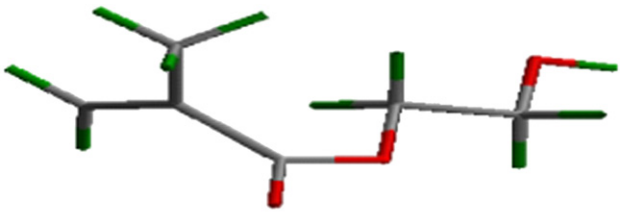

2-Hydroxyethyl methacrylate

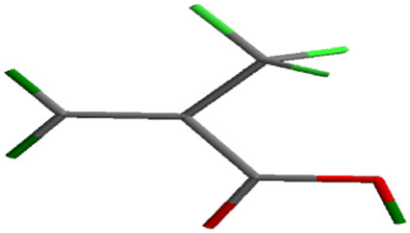

Trifluoro-methacrylic acid

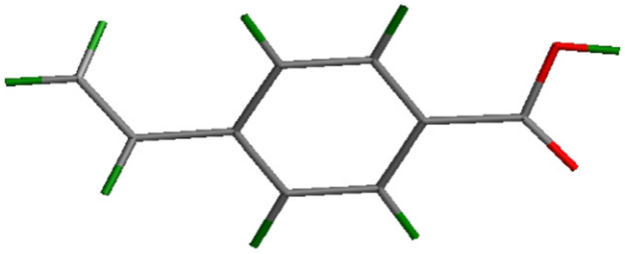

4-Vinylbenzoic acid

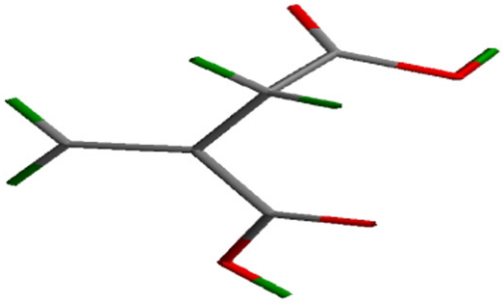

Itaconic acid

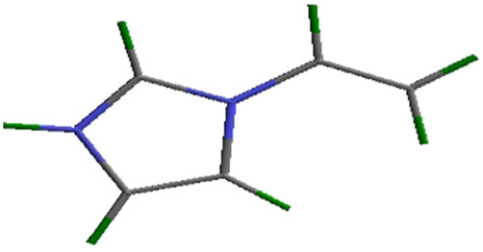

1-Vinylimidazole

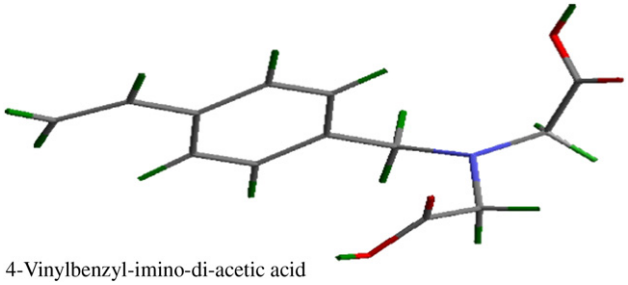

4-Vinylbenzyl-imino-di-acetic acid

References

[1] Pavel D, Lagowski J. Polymer 2005;46:7528–42.
[2] Pavel D, Lagowski J. Polymer 2005;46:7543.
[3] Lee W, Hara M, Lee H. Materials Science and Engineering C 2004;24:315–7.
[4] Toth R, Coslanich A, Ferrone M, Fermeglia M, Pricl SM, Chiellini E. Polymer 2004;45:8075–83.
[5] Kuijpers MWA, Iedema PD, Kemmere MF, Keurentjes JTF. Polymer 2004;6461–7.
[6] Zou R-Q, Bu X-H, Du M, Sui Y-X. Journal of Molecular Structure 2004;707:11–5.
[7] Chianella I, Piletsky SA, Tothill IE, Chen B, Turner APF. Biosensors and Bioelectronics 2003;18:119–27.
[8] Subrahmanyam S, Piletsky SA, Piletska EV, Chen B, Karim K, Turner PF. Biosensors and Bioelectronics 2001;16:631–7.
[9] Norell MC, Andersson HS, Nicholls IA. Journal of Molecular Recognition 1998;11:98–102; Takeuchi T, Haginaka J. Journal of Chromatography B 1999;728:1; Bruggemann O, Haupt K, Ye L, Yilmaz E, Mosbach K. Journal of Chromatography A 2000;889:15; Zimmerman SC, Lemcoff G. Chemistry Communications 2004;5.
[10] Ramanathan K, Pandey SS, Kumar R, Gulati A, Surya A, Murthy N, et al. Journal of Applied Polymer Science 2000;78:662–7.
[11] Carlqvist P, Eklund R, Hult K, Brinck T. Rational design of a lipase to accommodate catalysis of Baeyer–Villiger oxidation with hydrogen peroxide, vol. 9. Springer-Verlag; 2003. p. 164–71.
[12] Kaiser CT, Gubbens PCM, Kemner E, Overweg AR, Jayasooriya UA, Cottrell SP. Chemical Physics Letters 2003;381:292–7.
[13] Stevenson D. Trends in Analytical Chemistry 1999;18:154–8.
[14] Zheng N, Fu Q, Li Y-Z, Chang W-B, Wang Z-M, Li T-J. Microchemical Journal 2001;69:153–8.
[15] Reddy PS, Kobayashi T, Fujii N. European Polymer Journal 2002; 38:779–85.
[16] Pei K, Li Y, Li H. Journal of Molecular Structure 2003;660:113–8.
[17] Wu L, Sun B, Li Y, Chang W. Analyst 2003;128:944–9.
[18] Vasanthan N, Kotek R, Jung D-W, Shin D, Tonelli AE, Salem DR. Polymer 2004;45:4077–85.
[19] Tagowska M, Mazur M, Krysinski P. Synthetic Metals 2004;140:29–35.
[20] Cerius^2 simulation tool user's reference manuals, molecular simulation software for material science. San Diego, USA: Accelrys Inc.; 2004.
[21] Sun H. Journal of Computational Chemistry 1994;15:752–68.
[22] Sun H. Macromolecules 1994;26:5924–36.
[23] Sun H, Mumby SJ, Maple JR, Hagler AT. Journal of the American Chemical Society 1994;116:2978–87.
[24] Sun H. Macromolecules 1995;28:701–12.
[25] Pavel D, Yarovski I, Shanks R. Polymer 2005;46:2003–10.
[26] Brostow W. Science of materials. New York: John Wiley & Sons; 1979. p. 65.
[27] Rappe AK, Goddard III WA. Journal of Physical Chemistry 1991; 95:3358.
[28] Berendsen HJ, Postma JPO, van Gunsteren WI, Di Niola A, Haak JR. Journal of Chemical Physics 1984;81:3684.
[29] Sellergren B, Andersson LI. Methods 2000;22:92.
[30] Svenson J, Nicholls IA. Analytica Chimica Acta 2001;435:19.
[31] Theodoridis G, Manesiotis P. Journal of Chromatography A 2002; 948:163.
[32] Kim H, Spivak DA. Journal of the American Chemical Society 2003; 125:11269.
[33] Sellergren B. Macromolecules 2006;39:6306.
[34] Oral E, Peppas NA. Polymer 2004;45:6163.
[35] Nicholls IA. Journal of Molecular Recognition 1998;11:79.
[36] Wang R, Lai L, Wang S. Journal of Computer-Aided Molecular Design 2002;16:11.
[37] Tame JRH. Journal of Computer-Aided Molecular Design 1999;13:99.
[38] Lill MA, Vedani A, Dopler M. Journal of Medicinal Chemistry 2004; 47:6174.